

---

# Safety through feedback in Constrained RL

---

Shashank Reddy Chirra<sup>1</sup>, Pradeep Varakantham<sup>1</sup>, Praveen Paruchuri<sup>2</sup>  
Singapore Management University<sup>1</sup>, IIT Hyderabad<sup>2</sup>  
shashankc@smu.edu.sg, pradeepv@smu.edu.sg, praveen.p@iiit.ac.in

## Abstract

In safety-critical RL settings, the inclusion of an additional cost function is often favoured over the arduous task of modifying the reward function to ensure the agent's safe behaviour. However, designing or evaluating such a cost function can be prohibitively expensive. For instance, in the domain of self-driving, designing a cost function that encompasses all unsafe behaviours (e.g., aggressive lane changes, risky overtakes) is inherently complex, it must also consider all the actors present in the scene making it expensive to evaluate. In such scenarios, the cost function can be learned from feedback collected offline in between training rounds. This feedback can be system generated or elicited from a human observing the training process. Previous approaches have not been able to scale to complex environments and are constrained to receiving feedback at the state level which can be expensive to collect. To this end, we introduce an approach that scales to more complex domains and extends to beyond state-level feedback, thus, reducing the burden on the evaluator. Inferring the cost function in such settings poses challenges, particularly in assigning credit to individual states based on trajectory-level feedback. To address this, we propose a surrogate objective that transforms the problem into a state-level supervised classification task with noisy labels, which can be solved efficiently. Additionally, it is often infeasible to collect feedback on every trajectory generated by the agent, hence, two fundamental questions arise: (1) Which trajectories should be presented to the human? and (2) How many trajectories are necessary for effective learning? To address these questions, we introduce a *novelty-based sampling* mechanism that selectively involves the evaluator only when the agent encounters a *novel* trajectory, and discontinues querying once the trajectories are no longer *novel*. We showcase the efficiency of our method through experimentation on several benchmark Safety Gymnasium environments and realistic self-driving scenarios. Our method achieves near optimal performance (to when the cost function is known) just from gathering feedback at the trajectory level in many of the domains underscoring the effectiveness and scalability of our approach.

## 1 Introduction

Reinforcement Learning (RL) is known to suffer from the problem of reward design, especially in safety-related settings [4]. In such a case, constrained RL settings have emerged as a promising alternative to generate safe policies [3, 14, 32]. This framework introduces an additional cost function to split the task related information (rewards) from the safety related information (costs). In this paper, we address a scenario where the reward function is well-defined, while the cost function remains unknown *a priori* and requires inference from feedback. This arises in cases where the cost function is *expensive* to design or evaluate. For instance, consider the development of an autonomous driving system, where the reward function may be defined as the time taken to reach a destination which is easier to define. However, formulating the cost function presents significant challenges. Designing a comprehensive cost function that effectively penalizes all potential unsafe behaviors is non-trivial,

and ensuring safety often involves subjective judgments, which can vary based on the individual passenger preferences. Even if one succeeds in devising such a function, it must encapsulate data on all environmental factors, including neighboring vehicles and pedestrians. The evaluation of such a cost function in high-fidelity simulators can be prohibitively expensive.

The feedback can be collected from either a human observer, who monitors the agent’s training process and periodically provides feedback on presented trajectories, or from a system that computes the cost incurred on selected trajectories. Throughout this paper, we use the term *evaluator* to refer to the entity providing feedback, whether human or system-generated.

Cost inference in Constrained RL settings has gained recent attention. One key thread of research has focused on learning cost from from constraint abiding expert demonstrations [26, 30]. However, these expert demonstrations are not easily available in all settings. For example, consider robotic manipulation tasks where the human and the robot have different morphologies. This paper is focused on the second thread of research in this space, where we generate trajectories and take feedback from an evaluator to infer the cost function. Prior works in this thread make limiting assumptions on the nature of the cost function such as *smoothness* or *linearity* [26, 30, 10, 5] and are limited to obtaining feedback at the state level [7] which is expensive to collect from human evaluators. We do not make such assumptions and can take feedback provided at over longer horizons, in some cases the entire trajectory.

Frameworks for learning from feedback must exhibit the following properties to as emphasized in [7, 16, 11]: 1) The feedback must be collected *offline* in between rounds, since the agent may need to act in real time. 2) The framework should try to *minimize* the amount of feedback collected. 3) *Binary* feedback is more suitable as compared to *numeric* feedback as it is more intuitive to provide for humans. It has also been shown that humans provide less consistent feedback if it is *numeric* [11]. 4) Each state is assigned a binary cost value, indicating that it is inherently *safe* or *unsafe*, which is more intuitive for humans when assessing the safety of policies [29]<sup>1</sup>.

To this end we propose the **Reinforcement Learning from Safety Feedback (RLSF)** algorithm, which embodies all the aforementioned properties. The key contributions of this algorithm include:

- Extends prior work to collect feedback over longer horizons. This is done by presenting the evaluator with the entire trajectory, breaking the trajectory into segments and eliciting feedback at the segment level. Inferring the costs directly by *maximizing likelihood* presents new challenges due to the problem of credit assignment over longer horizons. To tackle this, we present a surrogate loss that converts the problem from trajectory level cost inference to a supervised binary classification problem with *noisy* labels.
- Introduces a *novelty based sampling* mechanism that reduces the number of queries by sampling *novel* trajectories for feedback.
- Learns safe policies across diverse benchmark safety environments. We also show that the learnt cost function can be used to train an agent with different dynamics/morphology from scratch without collecting additional feedback.

## 2 Preliminaries

**Markov Decision Process** A Markov Decision Process (MDP)  $\mathcal{M}$  is defined by the tuple  $(\mathcal{S}, \mathcal{A}, \mathcal{P}, r, \gamma, \mu)$ , where  $\mathcal{S}$  denotes the set of states,  $\mathcal{A}$  is the set of actions,  $\mathcal{P}(s'|s, a) \in [0, 1]$  is the transition probability,  $r(s, a) \in \mathbb{R}$  is the reward function,  $\gamma \in [0, 1]$  is the discount factor and  $\mu(s) \in \Delta(\mathcal{S})$  is the initial state distribution. A policy  $\pi(\cdot|s) \in \Delta(\mathcal{A})$  is a distribution over the set of valid actions for state  $s$ . We denote the set of all stationary policies as  $\Pi$ . A *trajectory*  $\tau = \{(s_t, a_t)\}$  denotes the state-action pairs encountered by following  $\pi$  in  $\mathcal{M}$ . We use the short hand  $\tau_{i:j}$  to denote a *trajectory segment*, i.e, the subsequence of  $(s_t, a_t)$  pairs encountered from timestep  $i$  to  $j$ . The *expected value* of a function  $f$  under  $\pi$  as  $\mathcal{J}^f(\pi) \triangleq E_{\tau \sim \pi}[\sum_{t=0}^{\infty} \gamma^t f(s_t, a_t)]$ . We also employ the shorthand  $f(\tau)$  to represent the discounted sum of  $f$  along the trajectory  $\tau$ . The occupancy measure of a policy is define as  $\rho(s, a) = E_{\tau \sim \pi}[\sum_{t=0}^{\infty} \gamma^t \mathbb{I}[(s_t, a_t) = (s, a)]]$ , where  $\mathbb{I}[\cdot]$  denotes the indicator function.  $\rho$  describes the frequency with which a state-action pair is visited by  $\pi$ .

<sup>1</sup>The last two points are specific to human evaluators

**Constrained Markov Decision Process** A Constrained MDP [4] introduces a function  $c(s, a) \in \mathbb{R}$  and a cost threshold  $c_{max} \in \mathbb{R}$  that defines the maximum cost that can be accrued by a policy. The set of feasible policies is defined as  $\Pi_c = \{\pi \in \Pi : \mathcal{J}^c(\pi) \leq c_{max}\}$ . A policy is considered to be *safe* w.r.t  $c$  if it belongs to  $\Pi_c$ .

### 3 Problem Definition

In this paper, we consider the constrained RL problem defined as,

$$\pi^* = \underset{\pi \in \Pi_c}{\operatorname{argmin}} \mathcal{J}^r(\pi) \quad (1)$$

We assume the threshold  $c_{max}$  is known, but the cost function is not known and must be inferred from feedback collected from an external evaluator. In many scenarios  $c_{max}$  is typically known, representing a predefined limit on acceptable costs or risks in the environment. However, crafting the cost function  $c(s, a)$  such that it penalizes all *unsafe* behaviour can be infeasible.

We incorporate an additional constraint enforcing the cost function to be binary, i.e,  $c(s, a) \in \{0, 1\}$ . This ensures that each state-action pair is inherently categorized as either *safe* or *unsafe*. We opt for this approach because it is simpler for human evaluators to assign a binary safety value to state-actions when assessing policy safety, as emphasized in [29].

### 4 Method

In this section, we introduce **Reinforcement Learning from Safety Feedback (RLSF)**, an on-policy algorithm that consists of two alternating stages: 1) Data/Feedback collection and 2) Constraint inference/Policy improvement. In the first stage, data is collected via rollouts of the current policy for a fixed number of trajectories. Next, a subset of these trajectories is presented for feedback from evaluator, which are then stored in a separate buffer. The second stage consists of two parts: i) Estimation of the cost function from the feedback data and ii) Improvement of the policy using the collected trajectories and their inferred costs. We repeat stages (1) and (2) until convergence.

First, we highlight how the feedback is collected and propose a method to infer the constraint function using this data. Next, we recognize the practical limitations of acquiring feedback for every trajectory during training and detail our approach to sampling a subset of trajectories for efficient cost learning of the cost function. Finally, we detail how the inferred cost function is used to improve the policy.

#### 4.1 Nature of the Feedback

In the feedback process, first the evaluator is shown the entire trajectory  $\tau_{0:T}$ . Post this, the trajectory is broken down into contiguous segments  $\tau_{i:j}$  of length  $k$  and feedback is obtained for each of these segments. Note that the segment length can be set based on the complexity of the environment. For simpler environments, feedback can be collected for the entire trajectory whereas for environments with long horizons and sparse cost violations feedback can be collected for shorter segments. This makes the problem of assigning credit to individual states less challenging. This approach is adopted by other works that rely on human feedback as well [11, 16]. Note that decreasing the segment length comes at a higher cost of obtaining feedback from the evaluator.

The evaluator is tasked with classifying a segment as *unsafe* if the agent encountered an *unsafe* state at any point during the segment. The decision was primarily driven by the aim to facilitate consistent feedback from the evaluator. Alternative approaches, such as categorizing the segment as *unsafe*, if a certain number of unsafe states are visited or leaving the classification upto subjective judgment of the evaluator were deemed prone to generating inconsistent feedback in the case of human evaluators [11].

#### 4.2 Inferring the Cost Function

Let  $P = \{\tau_{i:j}, y^{safe}\}$  be the feedback collected from the human, where  $y^{safe} = 1$  if the segment was labelled *safe* and vice-versa. We assume that there exists an underlying ground truth cost function  $c_{gt}(s, a) \in [0, 1]$  based on which the evaluator provides feedback. The probability that a state is

$safe$  is defined as  $p_{gt}^{safe}(s, a) = \mathbb{I}[c_{gt}(s, a) = 0]$ . By definition of how the feedback is collected, the probability that a trajectory segment  $\tau_{i:j}$  is labelled as  $safe$  is given by,

$$p_{gt}^{safe}(\tau_{i:j}) = \prod_{t=i}^j p_{gt}^{safe}(s_t, a_t) \quad (2)$$

Now, let  $p^{safe}(s, a)$  represent our estimate of  $p_{gt}^{safe}(s, a)$  that we intend to learn from the collected feedback. We can optimize  $p^{safe}(s, a)$  by minimizing the likelihood loss,

$$\begin{aligned} L^{mle} &= E_{(\tau_{i:j}, y^{safe}) \sim P} \left[ y^{safe} \log p^{safe}(\tau_{i:j}) + (1 - y^{safe}) \log 1 - p^{safe}(\tau_{i:j}) \right] \\ &= E_{(\tau_{i:j}, y^{safe}) \sim P} \left[ y^{safe} \log \prod_{t=i}^j p^{safe}(s_t, a_t) + (1 - y^{safe}) \log \left( 1 - \prod_{t=i}^j p^{safe}(s_t, a_t) \right) \right] \\ &= E_{(\tau_{i:j}, y^{safe}) \sim P} \left[ y^{safe} \sum_{t=i}^j \log p^{safe}(s_t, a_t) + (1 - y^{safe}) \log \left( 1 - \prod_{t=i}^j p^{safe}(s_t, a_t) \right) \right] \end{aligned} \quad (3)$$

Directly minimizing Eq 3 is challenging as the term  $\prod_{t=i}^j p^{safe}(s_t, a_t)$  would collapse to 0 when the segment length is long, causing unstable gradients. To address this issue, we propose using a surrogate loss function where we replace  $1 - \prod_{t=i}^j p^{safe}(s_t, a_t)$  by  $\prod_{t=i}^j (1 - p^{safe}(s_t, a_t))$ .

$$\begin{aligned} L^{sur} &= E_{(\tau_{i:j}, y^{safe}) \sim P} \left[ y^{safe} \sum_{t=i}^j \log p^{safe}(s_t, a_t) + (1 - y^{safe}) \sum_{t=i}^j \log (1 - p^{safe}(s_t, a_t)) \right] \\ &= E_{(\tau_{i:j}, y^{safe}) \sim P} \sum_{t=i}^j \sum_{s, a} \mathbb{I}[(s_t, a_t) = (s, a)] \left[ \mathbb{I}[y^{safe} = 1] \log p^{safe}(s, a) \right. \\ &\quad \left. + \mathbb{I}[y^{safe} = 0] \log (1 - p^{safe}(s, a)) \right] \\ &= E_{(s, a) \sim d_g} [\log p^{safe}(s, a)] + E_{(s, a) \sim d_b} [\log (1 - p^{safe}(s, a))] \end{aligned} \quad (4)$$

where  $d_g(s, a) = E_{(\tau_{i:j}, y_{safe}) \sim P} \left[ \sum_{t=i}^j \mathbb{I}[(s_t, a_t) = (s, a) \cap y^{safe} = 1] \right]$  and  $d_b(s, a) = E_{(\tau_{i:j}, y_{safe}) \sim P} \left[ \sum_{t=i}^j \mathbb{I}[(s_t, a_t) = (s, a) \cap y^{safe} = 0] \right]$  represent the densities with which states occur in  $safe$  and  $unsafe$  segments respectively.

The surrogate loss transforms the objective from the segment level, where issues of collapsing probabilities over lengthy segments arise, to the state level where we do not encounter this problem. Optimizing Eq 4 involves breaking down the segments into individual states and assigning each state the label of the segment. Subsequently, states are uniformly sampled at random, and the binary cross-entropy loss is minimized. Thus,  $L^{sur}$  represents a binary classification problem where one class contains *noisy* labels. Every *unsafe* state is always labelled correctly, as its occurrence forces the evaluator to label the segment *unsafe*. A *safe* state is correctly labeled *safe* when it appears in a segment labeled *safe* by the evaluator. However, if it occurs in a segment labeled *unsafe*, it is incorrectly labelled *unsafe*. We posit that with a sufficient number of samples, the number of correct labels will outweigh the number of incorrect labels for each state.

**Proposition 1.** *The surrogate loss  $L^{sur}$  is an upper bound on the likelihood loss  $L^{mle}$ .*

Thus, minimizing  $L^{sur}$  guarantees an upper bound on the likelihood loss of the estimated cost function.

Having discussed the surrogate loss, we now examine the characteristics of its optimal solution.

**Proposition 2.** *The optimal solution to Eq 4 yields the estimate,*

$$p_*^{safe}(s, a) = \frac{d_g(s, a)}{d_g(s, a) + d_b(s, a)} \quad (5)$$

Subsequently, we define the inferred cost function as  $c_*(s, a) \triangleq \mathbb{I}[p_*^{safe}(s, a) < \frac{1}{2}]$ . Employing  $c_*(s, a)$  in policy updates instead of  $c_{gt}(s, a)$  introduces a bias in estimating the cost accrued by the policy, that we analyse below. For this analysis, we assume that the feedback is *sufficient*, i.e. the density  $d(s, a)$  is greater than zero for every state, otherwise  $p^*(s, a)$  is not defined.

**Proposition 3.** *For a fixed policy  $\pi$ , the bias in the estimation of the incurred costs is given by,*

$$E_\pi[\gamma^t c_*(s, a)] - E_\pi[\gamma^t c_{gt}(s, a)] = E_{(s,a) \sim \rho_g^\pi} [\mathbb{I}[d_b(s, a) > d_g(s, a)]] \quad (6)$$

where  $\rho_g^\pi(s, a) = E_\pi[\sum_{t=0}^T \gamma^t \mathbb{I}[(s_t, a_t) = (s, a) \cap c_{gt}(s, a) = 0]]$  is the occupancy measure of safe states visited by  $\pi$ .

Proposition 3 highlights that  $c^*(s, a)$  mislabels some *safe* states as *unsafe* if their occurrence in segments labelled *unsafe* is higher than in segments labelled *safe* by the human evaluator. We argue that such occurrences are likely to decrease as more data is collected or with a reduced segment length, but recognize that it is guaranteed to be 0 only when the segment length is 1, i.e. feedback is received at the state-level.

Additionally, note that the bias is greater than or equal to 0, i.e. the expected cost  $E_\pi[c_*(s, a)]$  serves as an upper bound on the true cost incurred by  $\pi$ . Thus, ensuring that the policy does not exceed the threshold  $c_0$  on  $c_*$  guarantees that it adheres to the threshold on  $c_{gt}$ .

**Corollary 1.** *Any policy  $\pi$  that is safe w.r.t  $c_*$  is guaranteed to be safe w.r.t  $c_{gt}$ .*

In practice, we represent  $p_\theta^{safe}(s, a)$  using a neural network with parameters  $\theta$ . The resulting cost function is defined as  $c_\theta(s, a) \triangleq \mathbb{I}[p^{safe}(s, a) < \frac{1}{2}]$ .

### 4.3 Efficient Subsampling of Trajectories

To reduce the burden on the evaluator (and reduce the cost of feedback), we present a subset of the trajectories collected by the policy for feedback. The common approach is to break the problem into two parts: (1) define a schedule  $N_{queries}(i)$  that determines the number of trajectories to be shown to the user at the end of each data collection round  $i$ . Subsequently,  $N_{queries}(i)$  trajectories are sampled from those collected by the policy at data collection round  $i$ . While ideally, we aim to select the subset of trajectories maximizing the *expected value of information* [17], this task is computationally intractable [2]. To address this challenge, various sampling methods have been employed, seeking to maximize a surrogate measure of this value. Among these, *uncertainty sampling* stands out as the most prominent approach, wherein trajectories are sampled based on the estimator’s uncertainty about their predictions [11, 16, 18]. However, quantifying this uncertainty is non-trivial given the lack of calibration in neural network predictions. To address this challenge, ensemble methods are frequently employed where the disagreement among the models is used as an uncertainty measure. However, the training of  $n$  distinct neural networks can exact substantial resource costs, prompting consideration for alternative approaches

In light of this, we introduce a new form of *uncertainty sampling* called *novelty sampling*. With *novelty sampling*, we gather all the *novel* trajectories after each round and present them to the evaluator for feedback. Formally, we define a state as novel if its density in the feedback data collected so far  $d(s) = \sum_a d(s, a)$  is 0. A trajectory is deemed *novel* if it comprises of at least  $e$  novel states. This can be interpreted as ensuring the *edit distance* (a popular trajectory distance measure [25]) between the trajectory and previously seen trajectories is greater than  $e$ . We do consider novelty for state-action pairs as we found that extending to this case adversely impacted the performance.

The central notion is that the model is prone to errors on *novel* states- those it has not encountered during training. This arises because the policy evolves over time, venturing into states that were not previously encountered during data collection rounds. Hence, this sampling strategy effectively reduces the *epistemic uncertainty* of the model- error stemming from a lack of training data. Furthermore, this sampling method offers the advantage of implicitly establishing a decreasing querying schedule as novelty of trajectories reduces over time as shown in Figure 6 in the Appendix.

We compute the density  $d(s)$  through a count-based method, utilizing a hashmap to track the frequency of state occurrences in trajectories presented to the evaluator. Employing SimHash [9], we discretize the state space using a hash function  $\phi : S \rightarrow \{-1, 1\}^n$ , which maps *locally* similar states (measured by angular distance) to a binary code as:

$$\phi(s) = \text{sgn}(Ag(s)) \quad (7)$$

where  $g : S \rightarrow \mathbb{R}^d$  is an optional preprocessing function and  $A$  is an  $n \times d$  matrix with i.i.d entries drawn from a standard normal distribution. Also, note that  $n$  controls the granularity of the hash function, i.e. the number of states mapped to the same value. In our setting,  $g(s) = s$  as we observed no improvement when employing functions like autoencoders for feature extraction.

#### 4.4 Policy Optimization

Post the data collection round, where we sample trajectories  $\{\tau\}$  and their corresponding rewards  $\{r(\tau)\}$  using  $\pi$ , we estimate their costs  $c(\tau)$  using the inferred cost function. Our proposed method allows for the policy to be updated utilizing any on-policy constrained RL algorithm. In this study, we employ the PPO-Lagrangian algorithm[3] that combines the PPO algorithm [24] with a lagrangian multiplier to ensure safety.

A detailed description of the proposed method can be found in Algorithm 1. Lines [6-17] describe the data and feedback collection stage, and Lines [18-23] describe the cost inference and policy improvement stage.

---

#### Algorithm 1 Reinforcement Learning from Safety Feedback (RLSF)

---

```

1: Input: cost threshold  $c_0$ , segment length  $k$ , novelty criterion  $e$ 
2: Initialize: policy  $\pi_0$ 
3: Initialize: classifier  $c_\theta$ , learning rate  $lr_\theta$  and feedback buffer  $D$ 
4: Initialize:  $A \in \mathbb{R}^{n \times d}$  with entries sampled i.i.d from  $\mathcal{N}(0, 1)$ ,  $\phi(\cdot) = \text{sgn}(A^T(\cdot))$ , density map  $d(\cdot) \equiv 0$ .
5: while not converged do
6:   Collect trajectories  $\{\tau\}, \{r(\tau)\} \sim \pi$  ▷ Data Collection
7:   for each trajectory  $\tau^i \in \{\tau\}$  do ▷ Feedback Collection
8:     novel  $\leftarrow$  True if  $\exists$   $e$  states  $\{s_e\} \in \tau^i$  such that  $d(\phi(s_e)) > 0$ 
9:     if novel then
10:       Show  $\tau^i$  to the evaluator
11:       for each segment  $\tau_{j:j+k} \in \tau^i$  do
12:         Obtain feedback  $y^{safe}$  for the segment  $\tau_{j:j+k}^i$ .
13:          $D \leftarrow D \cup \{(s, a), y^{safe} \mid \forall (s, a) \in \tau_{j:j+k}^i\}$ 
14:          $d(\phi(s)) \leftarrow d(\phi(s)) + 1 \quad \forall s \in \tau_{j:j+k}^i$  ▷ Update the densities
15:       end for
16:     end if
17:   end for
18:   for each gradient step do ▷ Update cost estimates
19:     Sample random minibatch  $b \leftarrow \{(s, a), y_{safe}\} \sim D$ 
20:      $\theta \leftarrow \theta - lr_\theta \nabla L^{sur}(b)$ 
21:   end for
22:   Infer costs for  $\{c_\theta(\tau_i)\}$  for all  $\tau^i \sim \{\tau\}$ .
23:   Update  $\pi$  using  $\{r(\tau_i)\}$  and  $\{c_\theta(\tau_i)\}$ . ▷ Policy Improvement
24: end while

```

---

## 5 Experiments

We investigate the following questions in our experiments: 1) Does RLSF succeed in effectively learning safe behaviours? 2) Can the inferred cost function be transferred across agents in the same task? and 3) How does the proposed novelty based sampling scheme compare with other methods used in the literature?

### 5.1 Experiment Setup

We evaluate RLSF on multiple continuous control benchmarks in the Safety Gymnasium environment [15] and Mujoco simulator based environments introduced in [28]. The *Circle*, *Blocked Swimmer* and *Biased Pendulum* environments constrain the position of the agent whereas the *Half Cheetah*, *Hopper* and *Walker-2d* environments constrain the velocity of the agent. The *Goal* and *Push* tasks which are

Table 1: Performance of different algorithms on the Safety Benchmarks. The first 7 environments represent the *hard* constraint case. The remaining environments illustrate the *soft* constraint case, with values in brackets indicating the cost threshold. Each algorithm is run for 6 independent seeds.

Environment		Cost Known (Best Run)		Cost Inferred (Mean $\pm$ standard error)		
		PPOLag	SIMKC	SDM	SIM	RLSF (Ours)
Point Circle	Return	45.26	46.09	36.20 $\pm$ 3.95	22.26 $\pm$ 9.59	36.42 $\pm$ 1.78
	C.V Rate (%)	0.4	0.43	11.43 $\pm$ 0.69	35.21 $\pm$ 10.09	1.9 $\pm$ 0.09
Car Circle	Return	14.34	15.21	5.18 $\pm$ 2.48	6.34 $\pm$ 2.87	9.37 $\pm$ 0.97
	C.V Rate (%)	0.84	5.4	6.2 $\pm$ 6.18	4.53 $\pm$ 4.00	0.54 $\pm$ 0.30
Biased Pendulum	Return	717.43	983.27	495.58 $\pm$ 160.84	577.15 $\pm$ 184.31	721.48 $\pm$ 111.49
	C.V Rate (%)	0.0	0.1	39.91 $\pm$ 17.05	48.58 $\pm$ 21.67	0 $\pm$ 0
Blocked Swimmer	Return	22.62	21.05	86.96 $\pm$ 10.69	2.15 $\pm$ 8.58	16.09 $\pm$ 1.44
	C.V Rate (%)	3.91	0.01	92.8 $\pm$ 1.65	13.33 $\pm$ 12.11	0.01 $\pm$ 0.01
HalfCheetah	Return	2786.71	2497.82	3031.7 $\pm$ 336.48	257.34 $\pm$ 147.35	2112.63 $\pm$ 161.26
	C.V Rate (%)	0.42	0.06	59.4 $\pm$ 8.28	0.0 $\pm$ 0.0	0.06 $\pm$ 0.0
Hopper	Return	1705.00	1555.25	1097.57 $\pm$ 56.35	990.08 $\pm$ 8.66	1408.71 $\pm$ 27.3
	C.V Rate (%)	0.19	0.02	0.0 $\pm$ 0.0	0.0 $\pm$ 0.0	0.29 $\pm$ 0.018
Walker2d	Return	2947.25	2925.23	2195.94 $\pm$ 134.21	993.38 $\pm$ 17.69	2783.29 $\pm$ 57.51
	C.V Rate (%)	0.16	0.0	1.58 $\pm$ 1.53	0.0 $\pm$ 0.0	0.05 $\pm$ 0.01
Point Goal	Return	26.16	26.1	1.61 $\pm$ 1.8149	10.86 $\pm$ 4.1	24.65 $\pm$ 0.59
	Cost (40.0)	34.19	31.83	30.57 $\pm$ 13.29	52.76 $\pm$ 12.85	35.08 $\pm$ 1.08
Car Goal	Return	27.37	26.44	1.05 $\pm$ 2.83	10.88 $\pm$ 7.1	24.28 $\pm$ 2.1
	Cost (40.0)	41.67	35.41	34.71 $\pm$ 9.87	33.33 $\pm$ 11.26	41.25 $\pm$ 2.27
Point Push	Return	6.00	10.84	0.16 $\pm$ 0.14	3.63 $\pm$ 1.77	2.68 $\pm$ 1.03
	Cost (35.0)	26.08	26.96	22.89 $\pm$ 5.95	45.43 $\pm$ 3.86	30.51 $\pm$ 3.4
Car Push	Return	3.07	2.68	-3.04 $\pm$ 3.3	1.56 $\pm$ 0.46	1.54 $\pm$ 0.51
	Cost (35.0)	20.53	20.95	23.25 $\pm$ 7.78	36.55 $\pm$ 1.48	27.69 $\pm$ 1.19

the most challenging contain static and dynamic obstacles that the agent must avoid while completing the task. These environments represent safety challenges that an agent may encounter in the real world. Additionally, experiment on the Driver simulator introduced in [19] which introduces two scenarios that an autonomous driving agent is likely to encounter on the highway- the lane change and a blocked path. Here, the cost function considers multiple variables such as speed, position and distance to other cars. We also introduce a third scenario- overtaking in a two lane highway. A detailed description of the tasks can be found in the Appendix B.

We split the environments into two cases: (1) *hard constraint* case ( $c_{max} = 0$ ) where the safety of the policy is measured in terms of the cost violation (CV) rate defined as the average number of cost violations per state and (2) *soft* constraint case where  $c_{max} > 0$ . We use an automated script that uses the underlying cost function to simulate the feedback received from the evaluator.

We compare the performance of our algorithm against the following baselines: **Self Imitation Safe Reinforcement Learning (SIM)** [14]: SIM is a state-of-the-art method in constrained RL. It also supports the case where feedback is elicited from an external evaluator. Similar to RLSF, the method consists of two stages, a data collection/feedback stage and a policy optimization stage. In the first stage, a trajectory  $\tau$  is labelled as *good* if  $[r(\tau) \geq r_{good} \cap \mathbb{I}[c(\tau) \leq c_{max}]$ , and labelled as *bad* if  $[r(\tau) \geq r_{bad} \cup \mathbb{I}[c(\tau) \geq c_{max}]$ , where  $r_{good}$  and  $r_{bad}$  are predefined thresholds on the reward. The information  $\mathbb{I}[c(\tau) \leq c_{max}]$  is received from feedback. The idea is then to imitate the *good* trajectories and stay away from the *bad* trajectories. If  $\rho^\pi$  is the occupancy measure of the current policy  $\pi$  and  $\rho^G, \rho^B$  are the occupancy measures of the *good* and *bad* trajectories respectively, then,  $\pi$  is optimized as,

$$\pi^* = \operatorname{argmax}_{\pi} \operatorname{KL}(\rho^{\pi,G} || \rho^B) \quad (8)$$

where  $\rho^{\pi,G} = (\rho^\pi + \rho^G)/2$  and KL denotes the Kullback–Leibler divergence.

**Safe Distribution Matching (SDM)**: SIM combines rewards with safety feedback into a joint notion of *good* and *bad* which may not be desirable when the cost function is unknown. Thus, we introduce an additional baseline that keeps these two signals separate by labelling the trajectory as *good* if

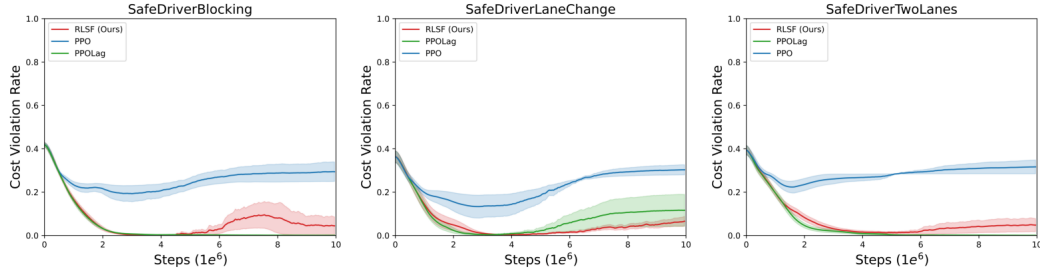


Figure 1: Cost Violation rate of different algorithms in driving environment. Each algorithm is run for 6 independent seeds, curves represent the mean and shaded regions represent the standard error.

$c(\tau) \leq c_{max}$  and *bad* otherwise. The policy is then updated as,

$$\pi^* = \operatorname{argmax}_{\pi} r + \lambda \text{KL}(\rho^{\pi, G} || \rho^B) \quad (9)$$

where  $\lambda \in [0, 1]$  controls the tradeoff between the two objectives.

As an upper bound, we compare the performance of our algorithm to the case where the cost function is known: PPO-Lagrangian (PPOLag) [3] and SIM with known costs (SIMKC) [14]. The goal here is not to beat their performance but to match them, hence when reporting the results of these algorithms we report the best performing seed across the different seeds.

All results presented use novelty-based sampling unless stated otherwise. We use a segment length of 1 in the *Driver*, *Goal* and *Push* environments. This is because the Safety Goal and Push environments contain small obstacles that the agent interacts with for very brief periods of time, hence requiring more fine-grained feedback. An example of this is present in Figure 8 in the Appendix. In the *Driver* environments, a randomly initialized policy was *highly unsafe*. Thus a long segment length would force the evaluator to label every segment *unsafe*, making cost inference infeasible. In all other environments, the segment length is equal to the length of the episode. Details on the number of queries generated for feedback can be found in Table 4 in the Appendix. We provide the two baseline methods (with unknown costs) with an advantage, whereby feedback is received for every trajectory generated.

## 5.2 Cost Inference across various tasks

**Benchmark Environments** Table 1 contains the performance of the different algorithms on the benchmark environments. RLSF significantly outperforms the two baselines in terms of reward and safety in *all* of the environments<sup>2</sup>. RLSF comes to within  $\sim 80\%$  of the performance of the best run of PPOLag in 7/11 environments thereby underscoring its effectiveness in learning safe policies.

**Driving Scenarios** We demonstrate the applicability of our method in learning safe autonomous driving policies. We compare the performance of our algorithm against two baselines: a naive PPO policy that solely maximizes reward and the PPO-Lag algorithm. Figure 1 presents these results. Notably, our method exhibits comparable safety performance to PPO-Lag and significantly outperforms the PPO in terms of cost violations. Video clips showcasing the learned policies in the 3 scenarios are included in the supplementary material.

## 5.3 Cost Transfer

We also demonstrate the potential of using the inferred cost to train a different agent to solve the same task from scratch and without additional feedback. We take the inferred cost function obtained during the training of a *Point* agent to solve the *Circle* and *Goal* tasks to train the *Doggo* agent. The observation space in the environments consists of agent-related telemetry (acceleration, velocity) and task-related information (lidar sensors for goal/boundary/obstacle detection). In these experiments we

<sup>2</sup>except the *Car Goal* environment where RLSF and PPOLag marginally exceed the threshold



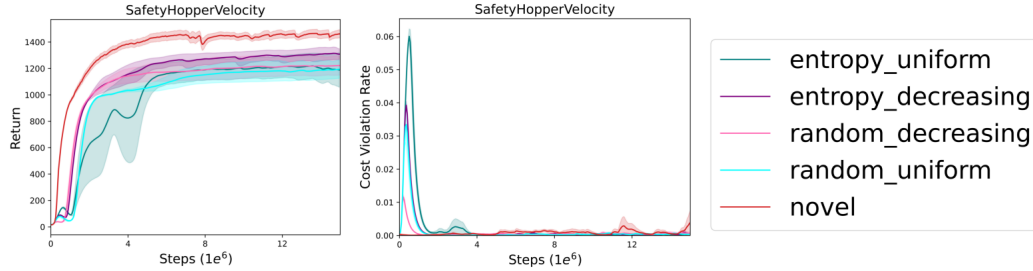


Figure 2: Comparison of different sampling and scheduling schemes. The results are averaged over 3 independent seeds. The proposed sampling method generates on average 1950 queries, hence for fair comparison the other methods were given a budget of 2000 queries.

do not use the agent-related information when learning the cost function, so that it can be transferred to a new agent. This cost function is kept fixed when training the second agent and the task-related features are used for cost-inference. We compare the performance of this approach with that of the PPO-Lagrangian algorithm that utilizes the underlying cost function of the environment. From Table 2 we can infer that agents trained using transferred cost function are comparable in performance to agents trained using the *unknown* underlying cost function.

Table 2: Comparison of the PPOLag when trained with the underlying task costs vs transferred costs. The results are averaged over 3 independent seeds.

Source Env	Target Env		PPOLag with true cost	PPOLag with transferred cost
Point Circle	Doggo Circle	Return	$2.69 \pm 0.24$	$2.00 \pm 0.27$
		C.V Rate (%)	$0.63 \pm 0.09$	$0.18 \pm 0.05$
Point Goal	Doggo Goal	Return	$1.45 \pm 0.06$	$1.20 \pm 0.26$
		Cost (40.0)	$40.86 \pm 4.80$	$37.31 \pm 6.77$

## 5.4 Ablation Study

Finally, we showcase the effectiveness of the proposed *novelty based sampling* mechanism. For this, we compare it against other querying mechanisms popular in the literature [16, 18]. These methods require a predefined budget on the number of trajectories to be shown to the evaluator. We compare against two schedules: (1) *Uniform schedule*: fixed number of trajectories shown for feedback after each round and (2) *Decreasing schedule*: number of trajectories shown decrease in proportion to  $\frac{1}{t}$  each round. For each schedule, we test the following strategies for sampling the subset of trajectories to be shown to the evaluator: (a) *Random sampling*: sample a random subset of trajectories and (b) *Entropy sampling*: Trajectories are sampled in descending order of average entropy  $\mathcal{H}(p_{\theta}^{safe}(s_t, a_t))$  of the estimator. From Figure 2, we can see that entropy based sampling outperforms random sampling, and a decreasing schedule outperforms a uniform schedule. However, all the methods fall short of the proposed *novelty based sampling* mechanism.

## 6 Limitations, Future Work and Broader Impact

Our method relies on state-level feedback in certain environments which can be costly if obtained from humans. While our theoretical results characterize the bias induced by collecting feedback for longer horizons, we do not explore explicit solutions to mitigate it. Investigating such solutions could enhance the performance of our method and is an interesting direction for future research. The proposed research has significant societal impacts. It can enable safer autonomous systems, potentially reducing accidents and enhancing road safety. However, reliance on learned cost functions can raise ethical concerns about accountability and liability.

## 7 Related Work

The Constrained Markov Decision Process (CMDP) framework [4] has emerged as a valuable tool in safety-critical settings, offering a clear separation between task-related information (rewards) and safety-related information (costs). This facilitates easier environment specification and transferability of the cost function across similar environments. While previous studies have extensively explored this problem [1, 33, 32, 14], they work under the assumption of a known cost function, which can pose limitations when designing the cost function is complex or its evaluation is expensive. Therefore, there arises a need to infer the cost function from external data sources in these cases.

In the past, cost inference has mainly been done from two types of data: 1) evaluator feedback and 2) constraint abiding expert demonstrations. Prior work in learning from feedback make limiting assumptions on the problem such as deterministic transitions and smoothness [26, 30, 10] or linearity assumptions [5] on the cost function. Also, none of these works consider the problem of actively querying the human in order to minimize the feedback required. This has been subsequently explored from a theoretical perspective in [7] but the proposed algorithm has yet to be adapted for complex environments. Also, these methods are limited to feedback collected for individual state action pairs which can be costly when working with human evaluators. We address these issues with our RLSF approach by intentionally reducing feedback required and making no assumptions on the cost function.

Inferring the cost from constraint satisfying expert demonstrations has received much attention recently [6, 31, 20]. However, these expert demonstrations can be difficult to acquire in many settings. Interventions are another type of feedback that can be collected from human evaluator. [21] rely on the human to terminate the episode when the agent is about to engage in *unsafe* behaviour while [23] rely on the human to take over control of the agent in such a scenario and lead it to a *safe* state. This work is also related to the analogous problem of reward inference in regular MDPs, which use similar types of data: human feedback [11, 16, 18] and expert demonstrations [13, 12].

Another related area is that of exploration: [8] introduced a pseudo-prediction task with the idea that states with high prediction errors indicate low visitation frequency due to *epistemic uncertainty*. [27] calculate state-density using Simhash [9] to provide an exploration bonus for states with low visitation frequency.

## References

- [1] J. Achiam, D. Held, A. Tamar, and P. Abbeel. Constrained policy optimization. *ArXiv*, abs/1705.10528, 2017.
- [2] N. Ailon. An active learning algorithm for ranking from pairwise preferences with an almost optimal query complexity. *J. Mach. Learn. Res.*, 13:137–164, 2010.
- [3] D. A. Alex Ray, Joshua Achiam. Benchmarking safe exploration in deep reinforcement learning, 2019.
- [4] E. Altman. *Constrained Markov Decision Processes*. Routledge, 1999.
- [5] S. Amani, C. Thrampoulidis, and L. F. Yang. Safe reinforcement learning with linear function approximation. *ArXiv*, abs/2106.06239, 2021.
- [6] U. Anwar, S. Malik, A. Aghasi, and A. Ahmed. Inverse constrained reinforcement learning. In *International Conference on Machine Learning*, 2020.
- [7] A. Bennett, D. K. Misra, and N. Kallus. Provable safe reinforcement learning with binary feedback. In *International Conference on Artificial Intelligence and Statistics*, 2022.
- [8] Y. Burda, H. Edwards, D. Pathak, A. Storkey, T. Darrell, and A. A. Efros. Large-scale study of curiosity-driven learning. In *International Conference on Learning Representations*, 2019.
- [9] M. S. Charikar. Similarity estimation techniques from rounding algorithms. In *Proceedings of the Thiry-Fourth Annual ACM Symposium on Theory of Computing*, STOC '02, page 380–388, New York, NY, USA, 2002. Association for Computing Machinery.
- [10] R. Cheng, G. Orosz, R. M. Murray, and J. W. Burdick. End-to-end safe reinforcement learning through barrier functions for safety-critical continuous control tasks. In *AAAI Conference on Artificial Intelligence*, 2019.
- [11] P. F. Christiano, J. Leike, T. B. Brown, M. Martic, S. Legg, and D. Amodei. Deep reinforcement learning from human preferences. *ArXiv*, abs/1706.03741, 2017.
- [12] D. Garg, S. Chakraborty, C. Cundy, J. Song, and S. Ermon. Iq-learn: Inverse soft-q learning for imitation. *ArXiv*, abs/2106.12142, 2021.
- [13] J. Ho and S. Ermon. Generative adversarial imitation learning, 2016.
- [14] H. Hoang, T. Mai, and P. Varakantham. Imitate the good and avoid the bad: An incremental approach to safe reinforcement learning, 2024.
- [15] J. Ji, B. Zhang, J. Zhou, X. Pan, W. Huang, R. Sun, Y. Geng, Y. Zhong, J. Dai, and Y. Yang. Safety gymnasium: A unified safe reinforcement learning benchmark. In *Thirty-seventh Conference on Neural Information Processing Systems Datasets and Benchmarks Track*, 2023.
- [16] K. Lee, L. M. Smith, and P. Abbeel. Pebble: Feedback-efficient interactive reinforcement learning via relabeling experience and unsupervised pre-training. In *International Conference on Machine Learning*, 2021.
- [17] J. S. Leonard. *The Foundations of Statistics*. John Wiley & Sons, 1978.
- [18] X. Liang, K. Shu, K. Lee, and P. Abbeel. Reward uncertainty for exploration in preference-based reinforcement learning, 2022.
- [19] D. Lindner, S. Tschitschek, K. Hofmann, and A. Krause. Interactively learning preference constraints in linear bandits, 2022.
- [20] G. Liu, Y. Luo, A. Gaurav, K. Rezaee, and P. Poupart. Benchmarking constraint inference in inverse reinforcement learning, 2023.
- [21] S. Poletti, A. Testolin, and S. Tschitschek. Learning constraints from human stop-feedback in reinforcement learning. In *Adaptive Agents and Multi-Agent Systems*, 2023.
- [22] D. Sadigh, A. D. Dragan, S. S. Sastry, and S. A. Seshia. Active preference-based learning of reward functions. In *Robotics: Science and Systems*, 2017.
- [23] W. Saunders, G. Sastry, A. Stuhlmüller, and O. Evans. Trial without error: Towards safe reinforcement learning via human intervention. In *Adaptive Agents and Multi-Agent Systems*, 2017.
- [24] J. Schulman, F. Wolski, P. Dhariwal, A. Radford, and O. Klimov. Proximal policy optimization algorithms, 2017.

- [25] H. Su, S. Liu, and B. Z. e. a. Zheng. A survey of trajectory distance measures and performance evaluation. *The VLDB Journal*, 29:3–32, 2020.
- [26] Y. Sui, A. Gotovos, J. Burdick, and A. Krause. Safe exploration for optimization with gaussian processes. In F. Bach and D. Blei, editors, *Proceedings of the 32nd International Conference on Machine Learning*, volume 37 of *Proceedings of Machine Learning Research*, pages 997–1005, Lille, France, 07–09 Jul 2015. PMLR.
- [27] H. Tang, R. Houthoofd, D. Foote, A. Stooke, X. Chen, Y. Duan, J. Schulman, F. D. Turck, and P. Abbeel. #exploration: A study of count-based exploration for deep reinforcement learning, 2017.
- [28] E. Todorov, T. Erez, and Y. Tassa. Mujoco: A physics engine for model-based control. In *2012 IEEE/RSJ International Conference on Intelligent Robots and Systems*, pages 5026–5033, 2012.
- [29] A. Wachi, W. Hashimoto, and K. Hashimoto. Long-term safe reinforcement learning with binary feedback, 2024.
- [30] A. Wachi and Y. Sui. Safe reinforcement learning in constrained markov decision processes. In *International Conference on Machine Learning*, 2020.
- [31] S. Xu and G. Liu. Uncertainty-aware constraint inference in inverse constrained reinforcement learning. In *The Twelfth International Conference on Learning Representations*, 2024.
- [32] L. Yang, J. Ji, J. Dai, L. Zhang, B. Zhou, P. Li, Y. Yang, and G. Pan. Constrained update projection approach to safe policy optimization. In S. Koyejo, S. Mohamed, A. Agarwal, D. Belgrave, K. Cho, and A. Oh, editors, *Advances in Neural Information Processing Systems*, volume 35, pages 9111–9124. Curran Associates, Inc., 2022.
- [33] Y. Zhang, Q. H. Vuong, and K. W. Ross. First order constrained optimization in policy space. *arXiv: Learning*, 2020.

## A Proofs

**Proposition 1.** *The surrogate loss  $L^{sur}$  is an upper bound on the likelihood loss  $L^{mle}$ .*

*Proof.* We have,

$$\begin{aligned} L^{sur} - L^{mle} &= -\frac{1}{|P|} \sum_{\tau_{i,j} \sim P} (1 - y^{safe}) \left[ \sum_{t=i}^j \log(1 - p^{safe}(s_t, a_t)) - \log\left(1 - \prod_{t=i}^j p^{safe}(s_t, a_t)\right) \right] \\ &= \frac{1}{|P|} \sum_{\tau_{i,j} \sim P} (1 - y^{safe}) \left[ \log\left(\frac{1 - \prod_{t=i}^j p^{safe}(s_t, a_t)}{\prod_{t=i}^j (1 - p^{safe}(s_t, a_t))}\right) \right] \end{aligned}$$

Notice that the term,

$$\log\left(\frac{1 - \prod_{t=i}^j p^{safe}(s_t, a_t)}{\prod_{t=i}^j (1 - p^{safe}(s_t, a_t))}\right) \geq 0$$

This is because

$$1 - \prod_{t=i}^j p^{safe}(s_t, a_t) \geq \prod_{t=i}^j (1 - p^{safe}(s_t, a_t))$$

which we prove subsequently.

**Lemma 1.** *For any sequence of numbers  $\{x_1, \dots, x_n\}$ , where  $x_i \in [0, 1]$  for all  $i \in 1, \dots, n$  we have  $1 - \prod_{i=1}^n x_i \geq \prod_{i=1}^n (1 - x_i)$ .*

*Proof.* Using the AM-GM inequality we have,

$$\begin{aligned} \sqrt[n]{\prod_{i=1}^n x_i} &\leq \frac{\sum_{i=1}^n x_i}{n} \\ 1 - \prod_{i=1}^n x_i &\geq 1 - \left(\frac{\sum_{i=1}^n x_i}{n}\right)^n \geq 1 - \left(\frac{\sum_{i=1}^n x_i}{n}\right) \end{aligned} \quad (10)$$

Similarly, we have,

$$\begin{aligned} \sqrt[n]{\prod_{i=1}^n (1 - x_i)} &\leq \frac{\sum_{i=1}^n (1 - x_i)}{n} \\ -\prod_{i=1}^n (1 - x_i) &\geq -\left(\frac{\sum_{i=1}^n (1 - x_i)}{n}\right)^n \geq -\left(\frac{\sum_{i=1}^n (1 - x_i)}{n}\right) \end{aligned} \quad (11)$$

Adding Eq 10 and Eq 11, we get,

$$\begin{aligned} 1 - \prod_{i=1}^n x_i - \prod_{i=1}^n (1 - x_i) &\geq 1 - \left(\frac{\sum_{i=1}^n x_i}{n}\right) - \left(\frac{\sum_{i=1}^n (1 - x_i)}{n}\right) \\ 1 - \prod_{i=1}^n x_i - \prod_{i=1}^n (1 - x_i) &\geq 0 \\ 1 - \prod_{i=1}^n x_i &\geq \prod_{i=1}^n (1 - x_i) \end{aligned} \quad (12)$$

□

□

**Proposition 2.** *The optimal solution to Eq 4 yields the estimate,*

$$p_*^{safe}(s, a) = \frac{d_g(s, a)}{d_g(s, a) + d_b(s, a)}$$

*Proof.* The proof is obtained by differentiating Eq 4 w.r.t  $p^{safe}(s, a)$  and setting it to 0.  $\square$

**Proposition 3.** *For a fixed policy  $\pi$ , the bias in the estimation of the incurred costs is given by,*

$$E_\pi[c_*(s, a)] - E_\pi[c_{gt}(s, a)] = E_{(s,a) \sim \rho_g^\pi}[\mathbb{I}[d_b > d_g]]$$

where  $\rho_g^\pi(s, a) = E_\pi[\sum_{t=0}^T \mathbb{I}[(s_t, a_t) = (s, a) \cap c_{gt}(s, a) = 0]]$  is the occupancy measure of true safe states visited by  $\pi$ .

*Proof.* The estimated cost function  $c_*(s, a) = \mathbb{I}[p_*^{safe}(s, a) < \frac{1}{2}]$ , from Eq 5 we get  $p_*^{safe}(s, a) < \frac{1}{2}$  when  $d_b(s, a) > d_g(s, a)$ . Thus,  $c_*(s, a) = \mathbb{I}[d_b(s, a) > d_g(s, a)]$ .

$$\begin{aligned} E_\pi[c_*(s, a) - c_{gt}(s, a)] &= E_{\tau \sim \pi} \sum_{t=0}^T [c_*(s_t, a_t) - c_{gt}(s_t, a_t)] \\ &= E_{\tau \sim \pi} \sum_{t=0}^T \sum_{s, a} \mathbb{I}[(s_t, a_t) = (s, a)] [c_*(s_t, a_t) - c_{gt}(s_t, a_t)] \\ &= E_{\tau \sim \pi} \sum_{t=0}^T \sum_{s, a} \left[ \mathbb{I}[(s_t, a_t) = (s, a) \cap c_{gt}(s, a) = 0] [c_*(s_t, a_t) - c_{gt}(s_t, a_t)] \right. \\ &\quad \left. + \mathbb{I}[(s_t, a_t) = (s, a) \cap c_{gt}(s, a) = 1] [c_*(s_t, a_t) - c_{gt}(s_t, a_t)] \right] \\ &= E_{\tau \sim \pi} E_{(s,a) \sim \rho_g^\pi} [c_*(s, a) - 0] + E_{(s,a) \sim \rho_b^\pi} [c_*(s, a) - 1] \end{aligned}$$

where  $\rho_g^\pi(s, a) = E_{\tau \sim \pi} [\sum_{t=0}^T \mathbb{I}[(s_t, a_t) = (s, a) \cap c_{gt}(s, a) = 0]]$  and  $\rho_b^\pi(s, a) = E_{\tau \sim \pi} [\sum_{t=0}^T \mathbb{I}[(s_t, a_t) = (s, a) \cap c_{gt}(s, a) = 1]]$ .

Note that when a state is *unsafe*, i.e,  $c_{gt}(s, a) = 1$ , then,  $p_*^{safe}(s, a) = 0$  as  $n_g(s, a) = 0$ . Thus for all of these states,  $c_*(s, a) = 1$ . Hence, we are left with,

$$\begin{aligned} E_\pi[c_*(s, a) - c_{gt}(s, a)] &= E_{(s,a) \sim \rho_g^\pi} [c_*(s, a)] \\ &= E_{(s,a) \sim \rho_g^\pi} [\mathbb{I}[d_b > d_g]] \end{aligned}$$

$\square$

**Corollary 2.** *Any policy  $\pi$  that is safe w.r.t  $c_*$  is guaranteed to be safe w.r.t  $c_{gt}$ .*

*Proof.* From Proposition 3, we know that  $E_\pi[c_*(s, a)] - E_\pi[c_{gt}(s, a)] = E_{(s,a) \sim \rho_g^\pi} [\mathbb{I}[d_b > d_g]]$ . Since  $E_{(s,a) \sim \rho_g^\pi} [\mathbb{I}[d_b > d_g]] \geq 0$ , we have  $E_\pi[c_*(s, a)] \geq E_\pi[c_{gt}(s, a)]$ .

Thus,  $E_\pi[c_*(s, a)] \leq c_0 \implies E_\pi[c_{gt}(s, a)] \leq c_0$ .  $\square$

## B Environments

### B.1 Benchmark environments:

**Mujoco** simulator [28] based environments extend the locomotion tasks to include safety constraints. The environments can be split into two types: position based constraints and velocity based, a detailed description is provide below:

1. **Position Based:** These environments are recent benchmarks introduced in [20]. Hence, we explain them in more detail.

- (a) *Blocked Swimmer*: The agent controls a robot that consists of three segments joined at two points. The goal is to move the agent towards the right by as fast as possible by the application of torque via rotors connected to the joints. The reward received after each time step is proportional to its motion in the  $X$ -direction during that timestep. The episode ends after 1000 timesteps is reached. It is easier for the agent to move to the right, hence to make the task challenging a cost is incurred if the  $X$  coordinate of the agent  $\geq 0.5$ , constraining the agent to the region  $-\infty \leq X < 0.5$ .
- (b) *Biased Pendulum*: The agents goal is to balance a pole on a cart. Each episode ends if the pole is dropped or a maximum of 1000 timesteps is reached. The agent receives a reward 1 when its  $X$ -coordinate lies in the region  $[\infty, 0.01]$  and monotonically decreases to 0.1 as at its  $X$  coordinate increases to 0 after which it receives a constant reward of 0.1, hence the agent is biased to move in the leftward direction. Consequently, a cost of 1 is incurred in the region  $(-\infty, -0.015]$  constraining the agent from moving too far left.

2. **Velocity Based:** These environments are a part of the Safety Gymnasium benchmarks. They add a constraint on the velocity of the *Half-Cheetah*, *Hopper* and *Walker-2d* agents respectively. The agent incurs a cost of 1 whenever it exceeds a threshold of  $v_{max}/2$ , where  $v_{max}$  is the maximum velocity that agent receives when trained by *PPO* for  $1e^7$  steps.

**Safety Gymnasium** [15] has emerged as a prominent benchmark when evaluating constrained RL algorithms, thus providing a challenging benchmark for cost inference. These environments consist of multiple agents such *Point*, *Car* and *Doggo*, listed in increasing order of the difficulty in controlling the agent. The goal is to complete a certain task using any one of these agents. In the *Circle* task, the agent must go around the boundary of a circle centered around the origin. However, the agent must do so while staying within a safe region which is characterized by two vertical boundaries located at  $x = \pm 0.7$ . A cost of 1 is incurred every time the agent is outside the confines of this boundary ( $|x| \geq 0.7$ ). In the *Goal* task, the agent must reach a designated goal area as soon as possible while simultaneously avoiding static and dynamic obstacles. A cost of 1 is incurred every time the agent collides with these obstacles. The *Push* task is similar to the *Goal* task with the added challenge that the agent must now push a block to the goal area while simultaneously avoiding collision with obstacles present in the environment.

## B.2 Safe Driver

Driving based environments are emerging as benchmarks for the problem of constraint inference [20], owing to the nuanced aspect of safety when it comes to driving. We test our algorithm on the *Driver* simulator introduced in [19, 22] to learn safe behaviours from feedback. This environment consists of two scenarios that a self driving agent is likely to encounter on the Highway: a blocked road and a lane change. We add another scenario that represents overtaking in a two lane highway, where the agent must overtake a slower car in its lane by using the second lane. This can be dangerous as the traffic in this lane is in the other direction and hence the agent must do so in a safe manner. We provide a brief description of the environment below.

The *Driver* environment used point-mass dynamic and consists of continuous state and action spaces. The state  $s_i$  of a vehicle in the simulation is described by the tuple  $(x, y, \phi, v)$ , that consists of the agent’s position  $(x, y)$ , heading  $\phi$  and velocity  $v$ . The observation of the *ego* vehicle consists of the concatenation of the states of all the vehicles in the scene. The environment takes two actions  $(a_1, a_2)$  where  $a_1$  represents the steering input  $a_2$  represents the applied acceleration.

The state of the agents evolves as,

$$s_{t+1} = (x + \delta x, y + \delta y, \phi + \delta \phi, v + \delta v)$$

$$(\delta x, \delta y, \delta \phi, \delta v) = (v \cos \phi, v \sin \phi, a_2 - \alpha v)$$

where  $\alpha$  is used to control the friction. Additionally, the velocity is clipped to the range  $[-1, 1]$  at each timestep.

The task is to control the *ego* vehicle (white in Figure 3) to reach the top of the road as soon as possible while adhering to costs on the velocity and distance to other vehicles. The trajectory of the other vehicles is fixed bar some random noise applied to its steering and acceleration inputs. The agent receives a reward  $r_t = 10(y_t - y_{t-1})$  every timestep, incentivizing it to cut through the traffic

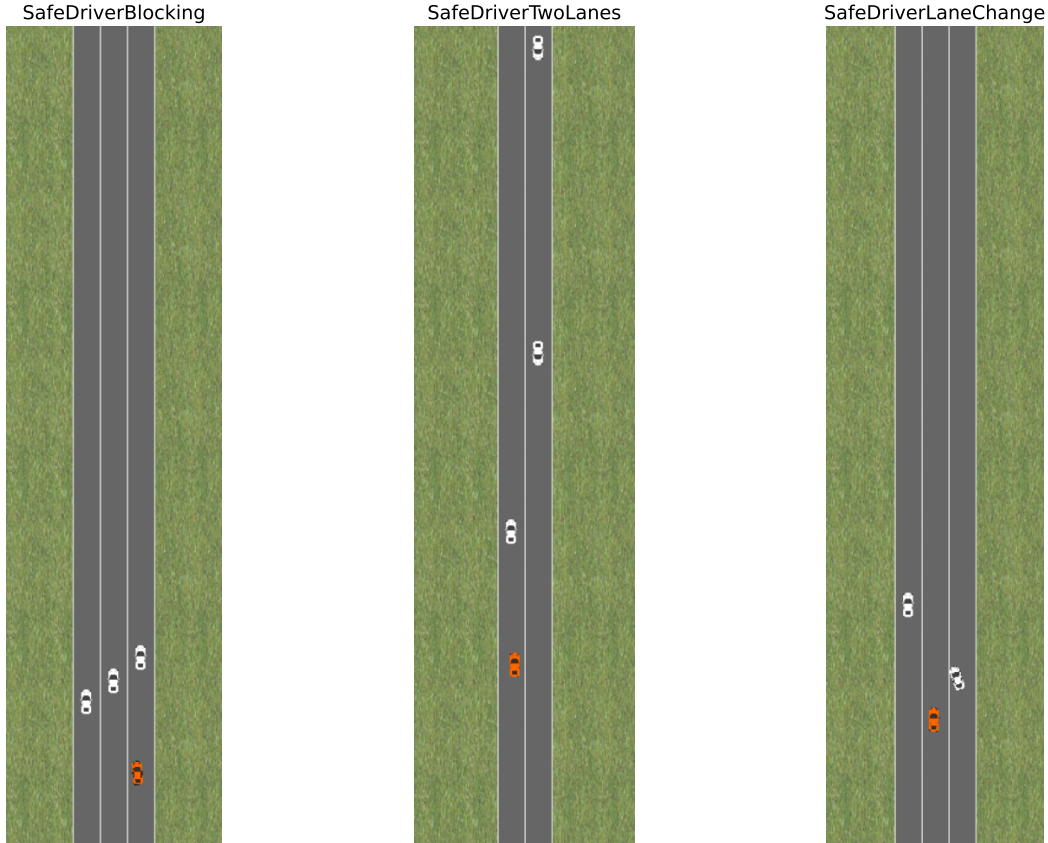


Figure 3: Driver Environments

as fast as possible. Additionally it receives a penalty  $-1$  if it goes off the road, drives backward or does not stay in the middle of the lane. It also incurs a penalty of  $-100$  for a collision. The episode is terminated if the agent reaches the top of the road or collides with another vehicle. We show that although such constraints can be incorporated into the reward function, it still leads to highly unsafe behaviour, highlighting the need for incorporating an additional cost function. The PPO agent is trained on this reward function.

In the CMDP settings, the cost function absorbs some of the constraints from the reward, i.e. the agent receives a cost of 1 when it goes off the road or drives backward. Additional costs are incurred when the agent crosses a speed limit  $v_{max}$  or gets too close to any nearby vehicle. The *ego* car is deemed to close to a neighbouring vehicle if  $\exp -b(c_1 d_x^2 + c_2 d_y^2) + ba \geq 0.4$ , where  $a = 0.01$ ,  $b = 30$ ,  $c_1 = 10$ ,  $c_2 = 2$  and  $d_x$  and  $d_y$  represent the distance of the nearby vehicle from the *ego* vehicle.

## C Experiments

### C.1 Hyperparameters

We conducted the experiments on a cluster containing 4 NVIDIA RTX A5000 GPUs and 96 core CPUs. The experiments took an approximate of two weeks to run. The detailed hyperparameters used in the experiments are reported in Table 3.



Table 3: Hyper Parameters

Hyper Parameter	Point Circle	Car Circle	Biased Pendulum	Blocked Swimmer	Half Cheetah	Hopper	Walker 2d	Point/Car Goal	Point/Car Push	Safe Driver
Actor hidden size	[256, 256, 256]	[256, 256, 256]	[256, 256, 256]	[256, 256, 256]	[256, 256, 256]	[256, 256, 256]	[256, 256, 256]	[256, 256, 256]	[256, 256, 256]	[64]
(Value/Cost) Critic hidden size	[256, 256, 256]	[256, 256, 256]	[256, 256, 256]	[256, 256, 256]	[256, 256, 256]	[256, 256, 256]	[256, 256, 256]	[256, 256, 256]	[256, 256, 256]	[64]
Classifier Network	[64,64]	[64,64]	[32]	[32]	[32]	[32]	[32]	[64, 64]	[64, 64]	[64]
Gamma	0.99	0.99	0.99	0.99	0.99	0.99	0.99	0.99	0.99	0.99
lr (Actor/Critic/Classifier)	0.0001	0.0001	0.0001	0.0001	0.0001	0.0001	0.0001	0.0001	0.0001	0.0001
lr Lagrangian	0.01	0.01	0.01	0.01	0.01	0.01	0.01	0.01	0.01	0.01
n_epochs (PPO/Critic)	160	160	160	160	160	160	160	160	160	160
n_epochs Classifier	5000	5000	5000	5000	5000	5000	5000	5000	5000	5000
Classifier batch size	4096	4096	4096	4096	4096	4096	4096	4096	4096	4096
SimHash Embedding size (k)	11	13	64	16	15	15	15	16	16	24

## C.2 Main Experiments

The training curves for the Benchmark experiments and the *Driver* environment are presented in Figure 4 and Figure 5. Additionally information on the number of queries presented for feedback is presented in Table 4.

Table 4: Number of Trajectories shown to the Evaluator for Feedback

Nature of Costs	Environment	Number of Trajectories shown	Episode Length	Segment Length ( $k$ )
Position	Point Circle	889.66 ± 185.27	500	500
	Car Circle	1063 ± 73.48	500	500
	Biased Pendulum	3939.33 ± 231.89	1000	1000
	Blocked Swimmer	646.83 ± 127.56	1000	1000
Velocity	HalfCheetah	4112.83 ± 134.26	1000	1000
	Hopper	1924.99 ± 92.59	1000	1000
	Walker2d	4170.33 ± 174.83	1000	1000
Obstacles	Point Goal	7892 ± 178.15	1000	1
	Car Goal	3866.5 ± 80.83	1000	1
	Point Push	6409.33 ± 77.46	1000	1
	Car Push	3368.33 ± 176.36	1000	1
Driving	Blocking	6242.3 ± 778.13	100	1
	Two Lanes	2912.37 ± 443.31	100	1
	Lane Change	3510.82 ± 644.28	100	1

## C.3 Novelty based Sampling

Figure 6 shows the implicit decreasing schedule encountered when using *novelty based sampling* in various environments. Figure 7 shows additional comparison with other querying mechanism in the Biased Pendulum environment.

## C.4 Number of Queries generated

The number of trajectories queried for feedback is of the order of  $\mathcal{O}(1e^3)$ , the exact number differs across environments and individual runs due to novelty based sampling. Detailed information on the number of queries can be found in Table 4. We provide the two baseline methods with an advantage, whereby feedback is obtained for every trajectory generated by the policy, which is of the order  $\mathcal{O}(1e^4)$ .

## C.5 Complexity of Constraint Inference

Figure 8 illustrates the challenge of inferring constraints when cost violations are sparse. Due to the brief interaction periods with obstacles in the environment, learning from feedback over longer horizons makes the problem of assigning credit to the *unsafe* states challenging. Therefore, feedback must be elicited at the state level becomes in such scenarios.

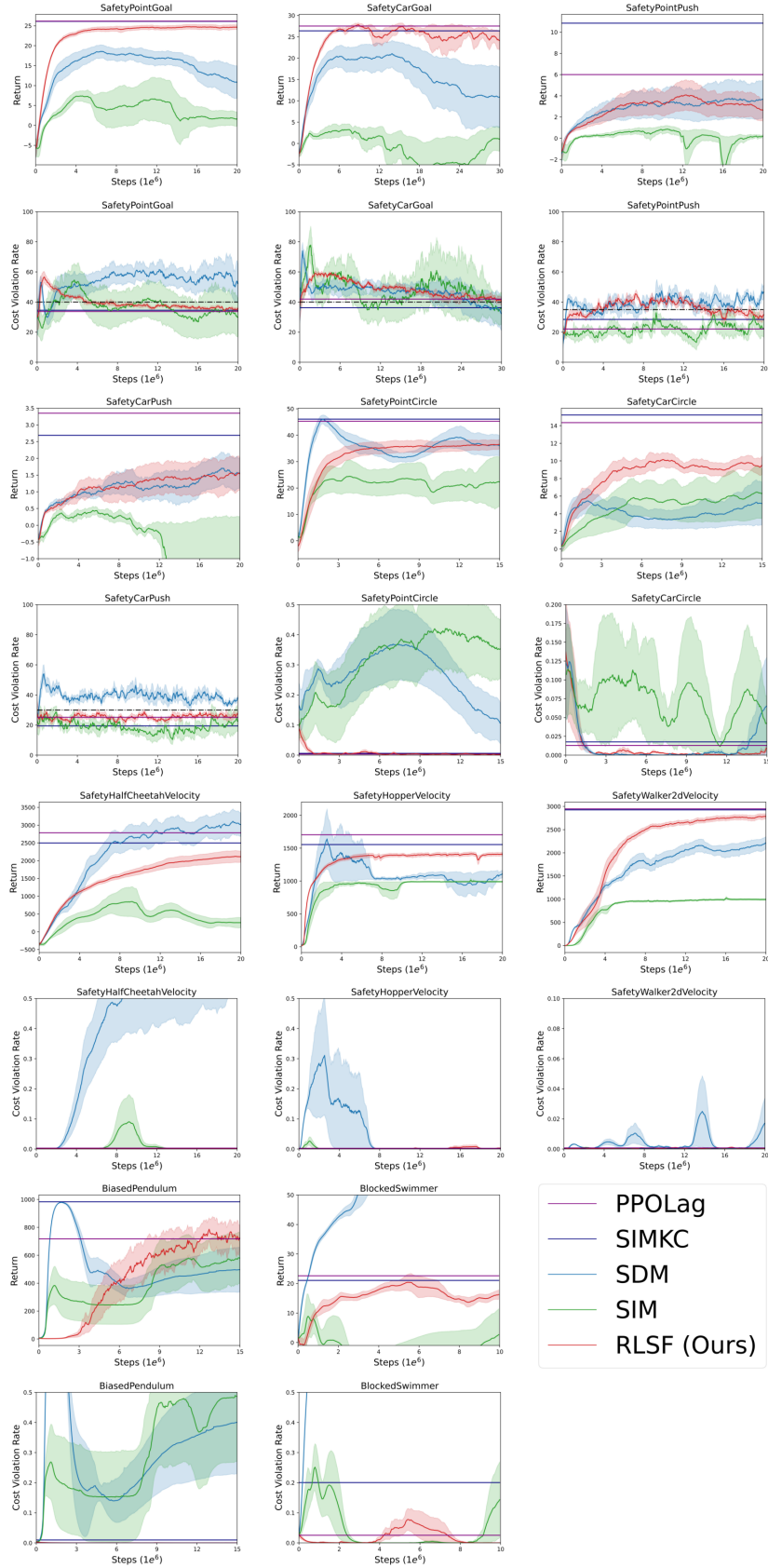


Figure 4: Training curves depicting the performance of different algorithms. The curves portray the mean returns, with shaded regions indicating the standard error. Parallel lines represents the best-performing run.

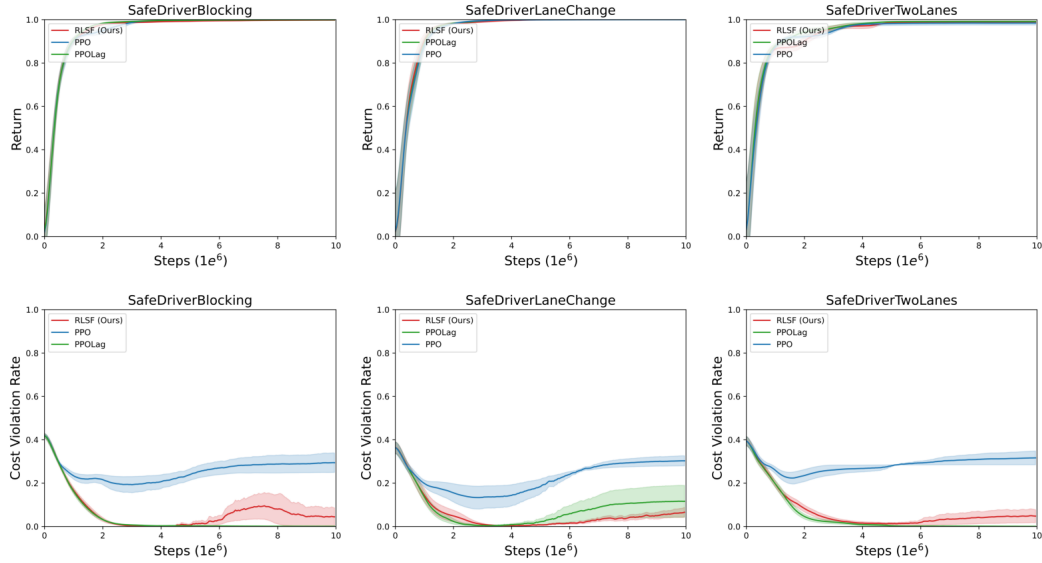


Figure 5: Performance of algorithms in different driving scenarios. Each algorithm is run for 6 independent seeds, curves represent the mean and shaded regions represent the standard error. Normalized return is given by the formula  $r = \frac{r - r_{\text{PPO}}}{r - r_{\text{random}}}$  where  $r_{\text{PPO}}$  is the return of PPO and  $r_{\text{random}}$  is the return of a random policy.

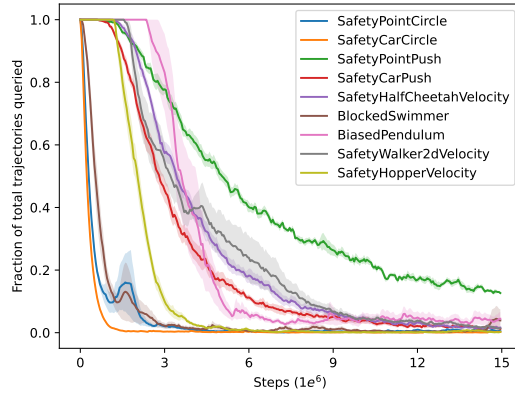


Figure 6: Implicit decreasing schedule observed when following novelty based sampling across different environments. The results are averaged over 6 independent seeds.

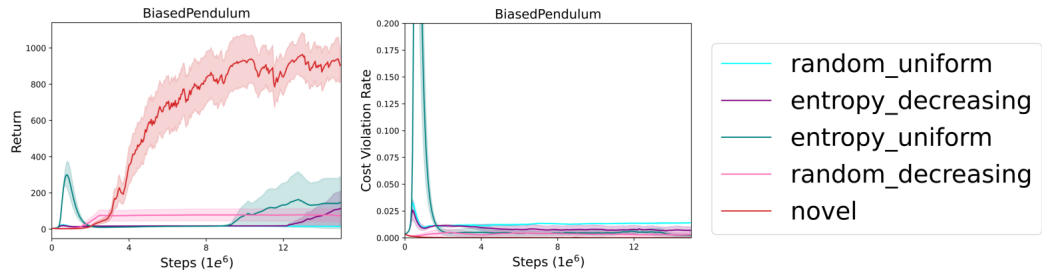


Figure 7: Comparison of different sampling and scheduling schemes. The results are averaged over 3 independent seeds. The proposed sampling method generates on average 3600 queries, hence for fair comparison the other methods were given a budget of 4000 queries.

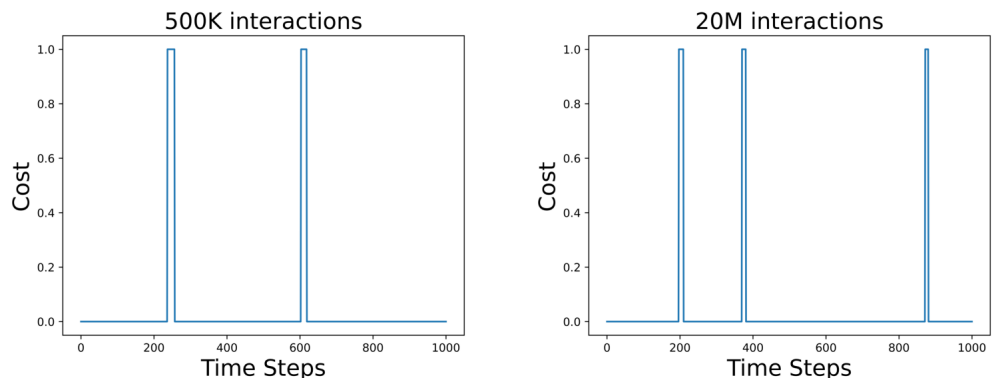


Figure 8: Costs incurred by a policy after 500K and 20M training interactions over a randomly sampled trajectory in the Point Goal environment.